

## From Dirac phenomenology to deuteron-nucleus elastic scattering at intermediate energies

A. Amorim and F. D. Santos

*Centro de Física Nuclear da Universidade de Lisboa, Avenida Gama Pinto 2, 1699 Lisboa, Portugal*

(Received 16 April 1991)

A discussion of relativistic microscopic models of deuteron-nucleus scattering at intermediate energies is presented. Calculations based on various relativistic models, which take into account explicitly the deuteron internal structure, and on the nonrelativistic folding model are compared with elastic-scattering data from  $^{40}\text{Ca}$  and  $^{58}\text{Ni}$  at 400 and 700 MeV. The same global nucleon-nucleus Dirac optical potentials were used throughout. We find that the direct impulse approximation, where the deuteron-nucleus  $T$  matrix is the expectation value of the sum of the nucleon-nucleus  $T$  matrices in the deuteron, gives a reasonable description of the data. However, the fact that the best agreement is provided by the nonrelativistic folding model indicates the need for a more realistic treatment of multiple scattering and off-shell effects in the relativistic microscopic models.

### I. INTRODUCTION

Proton-nucleus elastic scattering at intermediate energies has been successfully analyzed in recent years using relativistic models based on the Dirac equation [1]. In phenomenological approaches the nuclear optical potential consists of two terms, one a Lorentz scalar and the other a timelike component of a four-vector. This type of potential is able to reproduce proton elastic-scattering data, including the polarization observables, over a wide range of energy and mass number.

It is therefore desirable to extend the application of relativistic dynamics to composite nuclei. The deuteron is obviously a particularly interesting case because its loosely bound structure suggests that deuteron-nucleus scattering can be described in terms of free nucleon-nucleus scattering. The simplest way to approach this problem is to consider the deuteron as a relativistic pointlike spin-1 particle. However, unlike the case of spin- $\frac{1}{2}$ , there are various spin-1 relativistic wave equations [2-4]. Calculations of deuteron elastic-scattering observables using these equations have been performed and a recently reported comparison between their predictions [5], using the same nucleon-nucleus potentials, shows that there are no significant differences. However, the strength of the spin-orbit potential tends to be too weak and consequently the magnitudes of the vector analyzing power  $A_y$  and the tensor analyzing power  $A_{yy}$  are considerably smaller than the experimental data.

In a previous paper [6] we have shown that when a Dirac spinor structure is attributed to a nonrelativistic deuteron bound-state wave function, consistently with the Bethe-Salpeter formalism, and furthermore we allow for a relative internal momentum in this structure, the predicted effective spin-orbit interaction is stronger and has the expected  $d(V-S)/dr$  form. On the other hand, a weaker spin-orbit potential with the anomalous  $-dS/dr$  form is obtained by neglecting the dependence of the Dirac spinors on the deuteron internal momentum. These results indicate that a coherent relativistic and mi-

croscopic description of deuteron-nucleus scattering must take into account the two-nucleon Dirac structure of the deuteron.

In recent years it has been possible to deduce the proton-nucleus Dirac potentials, either from the nuclear  $T$  matrix in a suitable covariant parametrization [7] or, with improved results, from an ambiguity free calculation of the nucleon-nucleus amplitude [8]. These calculations use a special form of the relativistic impulse approximation in which the proton-nucleus potentials are obtained from folding the nucleon-nucleon  $T$  matrix over the nuclear wave function. It is assumed that this procedure introduces the relevant aspects of multiscattering effects into proton-nucleus scattering. One of the purposes of the present work is to apply a similar type of approximation to deuteron-nucleus scattering.

From the theoretical viewpoint deuteron-nucleus scattering is a complicated many-body problem. The calculation of the scattering amplitude should involve explicitly all the nucleons with the appropriate boundary conditions of a bound deuteron and a bound nucleus in the asymptotic states. This calculation is virtually impossible and the use of optical potentials allow us to introduce effectively the nucleus structure into the problem. In the optical potential approximation deuteron-nucleus scattering becomes a three-body problem and therefore we should consider explicitly the possibility of deuteron breakup.

The relativistic problem is still more complicated as no coupled-channel prescription is available, the off-shell behavior of the optical potential is not well defined, and the Dirac structure of the two-nucleon intermediate states has to be considered in all frames due to the recoil of the nucleus.

The results of Ref. [6] and the question of covariance in the calculations are discussed in Sec. II. In Sec. III we consider the nucleon-nucleus  $T$  matrix which is needed to formulate the relativistic impulse approximation. The deuteron-nucleus scattering equation is examined in Sec. IV. A theoretical discussion of different forms of the impulse approximation and their relations to the exact

theory will be presented in Sec. V. In Sec. VI the expressions of the nonrelativistic folding model in momentum space are introduced. Calculations and the discussion of the results are presented in Secs. VII and VIII.

## II. RELATIVISTIC FOLDING OF THE NUCLEON-NUCLEUS OPTICAL POTENTIALS

The proton-nucleus interaction is represented in the form frequently used in phenomenological analysis [1], namely,

$$U = S + \gamma^0 V, \quad (2.1)$$

where  $S$  and  $V$  are scalar and vector potentials assumed to be local. This expression for  $U$  is noncovariant and therefore it is only valid in a particular reference frame. Due to the presence of a second nucleon which shares the total deuteron momentum, the folding procedure should, in principle, be performed with a covariant expression for the proton-nucleus interaction. A natural covariant generalization of  $U$ , which reduces to the previous expression in the center-of-mass frame, is

$$U = S + \frac{V}{\sqrt{s}} \mathbf{P}, \quad (2.2)$$

where  $P^\mu$  is the total four-momentum given by the sum of the proton momentum  $p^\mu$  and the target-nucleus momentum  $P_N^\mu$  and  $s$  is the invariant center-of-mass energy. Another possible covariant form for  $U$  is

$$U = S + \frac{V}{M_N} \mathbf{P}_N, \quad (2.3)$$

where  $M_N$  is the target-nucleus mass. This expression leads to the noncovariant form (2.1) in the laboratory frame. The vector part in Eqs. (2.2) and (2.3) corresponds to the boost of a four-vector potential  $V^\mu$  that only in a particular reference frame has the form  $V^\mu = (V, 0)$ .

The use of the Dirac equation, which is a one-body equation, in the description of proton-nucleus scattering implies necessarily that the effects due to the recoil of the target nucleus must be taken into account in an approximate way [9]. In other words, the Dirac equation must be solved using the interaction  $U$  in a particular reference frame. We follow here the usual assumption that the laboratory frame coincides with the center-of-mass frame which is a more reliable approximation for heavier target nuclei. Thus  $P^\mu \approx P_N^\mu$  and  $U$ , as given by either Eq. (2.2) or (2.3) reduces to the form of Eq. (2.1) in the laboratory frame.

In Ref. [6] the deuteron-nucleus effective interaction was generated by folding the nucleon-nucleus interaction (2.1) over a relativistic model of the deuteron internal wave function, which was taken to be a pure  $^3S_1$  state. In momentum space the resulting potential has the form

$$U_d = U_c(q) + iU_{s.o.}(q) \mathbf{J} \cdot (\mathbf{P}'_d \times \mathbf{P}_d), \quad (2.4)$$

where  $\mathbf{J}$  is the spin-1 operator,  $\mathbf{P}_d$  and  $\mathbf{P}'_d$  are the initial and final deuteron momenta, and  $q = |\mathbf{P}'_d - \mathbf{P}_d|$  is the magnitude of the transferred momentum. Under the as-

sumption that the nucleon-nucleus interaction is isospin invariant the central and spin-orbit parts of the relativistic deuteron potential are related to  $S$  and  $V$  by the equations [6]

$$U_c(q) = \frac{[(E_d + M_d)(E_d^{\text{int}} + M_d)]^{1/2}}{2M_d} \times \left[ 2\rho(V + S) + (V - S) \frac{2(P_d^2 - q^2)\rho + 8q^2\rho''}{(E_d + M_d)(E_d^{\text{int}} + M_d)} \right] \quad (2.5)$$

and

$$U_{s.o.}(q) = \frac{2\rho(V - S)}{M_d[(E_d + M_d)(E_d^{\text{int}} + M_d)]^{1/2}}. \quad (2.6)$$

Here  $M_d$  is the deuteron mass,  $E_d$  is the deuteron energy, and  $E_d^{\text{int}}$  is related to the energy of the interacting nucleon and is given by Eq. (3.27) of Ref. [6].  $\rho$  is the deuteron probability density and  $\rho''$ , given by Eq. (3.22) of Ref. [6], is proportional to the expectation value of the deuteron internal kinetic energy. Both  $\rho$  and  $\rho''$  are in momentum space and calculated at half the transferred momentum.

The Dirac potentials  $S$  and  $V$  have a smooth energy dependence [10] which, in our case, must be considered carefully since the nucleon is no longer on mass shell. In fact, the integration over the deuteron relative momentum should in principle involve the energy dependence in  $S$  and  $V$ . However, the deuteron total momentum and kinetic energy are much larger than the relative momentum and binding energy. Thus the nucleon-nucleus potential will be considered constant and equal to its value at half the deuteron energy. Furthermore, the dependence of the deuteron potential on the total momentum is removed through the use of the asymptotic relation  $\mathbf{P}_d^2 = E_d^2 - M_d^2$  which is assumed to be also valid in the intermediate states. With these approximations the nonlocal character of the potential is removed. This simplifies considerably the calculation of the potentials  $U_c$  and  $U_{s.o.}$  in configuration space. The deuteron-nucleus central potential  $U_c(R)$  was obtained by Fourier transforming  $U_c(q)$  while the spin-orbit potential is given by

$$U_{s.o.}(R) = \frac{1}{R} \frac{d}{dR} \frac{1}{2\pi^2} \int_0^\infty q dq \frac{\sin(qR)}{R} U_{s.o.}(q), \quad (2.7)$$

according to Appendix C of Ref. [6].

In the low-energy limit we find that the strength of  $U_{s.o.}(R)$  is in good agreement with the nonrelativistic deuteron folding model. The crucial reason for this agreement [6] is that  $U_{s.o.}(q)$  depends on the linear combination  $V - S$  which is also present in the effective nucleon-nucleus spin-orbit potential.

The effective deuteron potential  $U_c$  depends linearly on the nucleon-nucleus scalar and vector potentials  $S$  and  $V$ . On the other hand, we know that when the Dirac equation is reduced to Schrödinger form the effective nucleon-nucleus central potential contains a quadratic dependence on  $S$  and  $V$  through a term proportional to

$S^2 - V^2$ . This term plays an important role in proton-nucleus elastic scattering and is responsible for the energy-dependent wine-bottle shape of the central potential. We may therefore expect that the use of the potential given by Eq. (2.4) will not provide a realistic description of deuteron-nucleus scattering observables over an extended energy range. Quadratic terms in  $S$  and  $V$  are present in effective deuteron-nucleus central potentials derived, after reduction to Schrödinger form, from one-body relativistic spin-one equations where the potentials  $S$  and  $V$  are introduced by minimal coupling [2–5].

An alternative approach, that we shall follow here, is to generate the deuteron-nucleus potential directly from the nucleon-nucleus  $T$  matrix. In this way the effects of the quadratic terms in  $S$  and  $V$  are included in the deuteron interaction.

### III. THE NUCLEON-NUCLEUS $T$ MATRIX

In order to construct the nucleon-nucleus  $T$  matrix we shall now consider a covariant parametrization for the special case where a nucleon is scattered from a spin-zero nucleus. Parity conservation implies that there are eight independent invariant amplitudes which is half the number of degrees of freedom present in the product of the initial and final states. There are three independent momenta which may be chosen as the total momentum  $P^\mu$  and the nucleon initial- and final-state momenta  $p^\mu$  and  $p'^\mu$ . Using the projection operators into negative-energy states  $\Lambda = (m - \not{p})/2m$  and  $\Lambda' = (m - \not{p}')/2m$ , the  $T$ -matrix expansion can be written as

$$T = T_s + T_0 \Gamma^0 + T_1 \Lambda + T_2 \Lambda' + T_3 \Gamma^0 \Lambda + T_4 \Lambda' \Gamma^0 + T_5 \Lambda' \Lambda + T_6 \Lambda' \Gamma^0 \Lambda, \quad (3.1)$$

where  $\Gamma^0 = \mathbf{P}/\sqrt{s}$ . The relation between this parametrization and the noncovariant parametrization used in the proton-nucleus relativistic impulse approximation [8] is readily established considering a special reference frame. To calculate the eight amplitudes  $T_k$  one needs to compute the lower and upper components of the Dirac scattering wave function so that the matrix elements involving the negative- and positive-energy Dirac spinors can be determined.

Instead of calculating the  $T_k$  we specify a particular covariant expression for the  $T$  matrix following the model used in the relativistic impulse approximation for proton-nucleus scattering of McNeil, Shepard, and Wallace [7]. This corresponds to the minimal relativity approximation where only terms that do not depend on the proton momentum are kept. Thus we write

$$T = T_s(s_i) + T_0(s_i) \Gamma^0, \quad (3.2)$$

where  $s_i$  are the six independent invariants constructed with the momenta  $p$ ,  $p'$ , and  $P$ . Neglecting recoil effects and considering the nucleons on mass shell we can write the proton-nucleus  $T$  matrix as

$$T = T_s(s, q) + T_0(s, q) \gamma^0. \quad (3.3)$$

As in Sec. II we use in our folding procedure the ampli-

tudes calculated at half the deuteron energy thereby removing the nonlocal character of the interaction.

To calculate the  $T$ -matrix amplitudes  $T_s$  and  $T_0$  we first solve the Dirac equation, with the potentials  $S + \gamma^0 V$ , in the usual way through its reduction to a Schrödinger-type equation for the upper components. The  $T$  matrix for this equation has the general form

$$T_f(\theta) + i \sigma_n T_g(\theta), \quad (3.4)$$

where  $\sigma_n = \sigma_n \cdot \mathbf{n}$  is the projection of the Pauli spin operator perpendicular to the reaction plane. Since the  $T$  matrix of Eq. (3.4) is obtained for the positive-energy Dirac states and with the nucleons on mass shell we write

$$\bar{u}_\sigma(\mathbf{p}') (T_s + \gamma^0 T_0) u_\sigma(\mathbf{p}) = T_f + i (\sigma_n)_{\sigma, \sigma'} T_g, \quad (3.5)$$

where the positive-energy Dirac spinors  $u$  are normalized according to  $\bar{u}u = 1$ . Solving with respect to  $T_s$  and  $T_0$  on mass shell, in the case of elastic scattering, we obtain

$$T_s = \frac{m}{E_p + m} \left[ T_f + \frac{D + (E_p + m)^2}{C} T_g \right], \quad (3.6)$$

$$T_0 = \frac{m}{E_p + m} \left[ T_f + \frac{D - (E_p + m)^2}{C} T_g \right], \quad (3.7)$$

where  $E_p$  is the proton energy,  $D = \mathbf{p} \cdot \mathbf{p}'$ , and  $C = |\mathbf{p}' \times \mathbf{p}|$ . In calculating  $T_s$  and  $T_0$  we have assumed that  $\mathbf{p}^2 = \mathbf{p}'^2 = (E_d/2)^2 - m^2$ . This corresponds to the usual choice of the Breit frame as in the calculation of the proton-nucleus optical potential using the relativistic impulse approximation.

The normalization in Eq. (3.5) is chosen in such a way that in the limit of very weak potentials the Born approximation corresponds to  $T_s = S$  and  $T_0 = V$ . It is shown in Appendix A that the calculation of the observables in the relativistic formalism reproduces the corresponding non-relativistic expressions.

In the impulse approximation the lowest-order scattering amplitude results from the coherent scattering by the individual nucleons in the deuteron, regarded as free but distributed in space according to the deuteron internal density. In this approximation the deuteron-nucleus  $T$  matrix is given by

$$\langle \mathbf{P}'_d, m'_d | T_d | \mathbf{P}_d, m_d \rangle = \langle \psi_{\mathbf{P}'_d, m'_d} | T_1 + T_2 | \psi_{\mathbf{P}_d, m_d} \rangle, \quad (3.8)$$

where  $\psi_{\mathbf{P}_d, m_d}$  represents the deuteron internal wave function with momentum  $\mathbf{P}_d$  and spin projection  $m_d$  and  $T_1, T_2$  are the nucleon-nucleus  $T$  matrices given by Eq. (3.3). Equation (3.8) describes the simplest form of the relativistic impulse approximation and will be denoted as the direct impulse approximation. The resulting deuteron-nucleus  $T$  matrix, after folding, has the form of Eq. (2.4) with  $S$  and  $V$  replaced by  $T_s$  and  $T_0$  in Eqs. (2.5) and (2.6).

The simplest relation between the deuteron-nucleus effective optical potential  $U_d$  and  $T_d$  is given by the Born approximation where

$$\langle \mathbf{P}'_d, m'_d | U_d | \mathbf{P}_d, m_d \rangle = \langle \psi_{\mathbf{P}'_d, m'_d} | T_1 + T_2 | \psi_{\mathbf{P}_d, m_d} \rangle. \quad (3.9)$$

This model is currently used in the application of the relativistic impulse approximation to proton-nucleus scattering [8]. In that case the proton-nucleus effective interaction is given by the expectation value of a sum of nucleon-nucleon  $T$  matrices in the target-nucleus ground state. This procedure neglects nuclear-medium modifications of the  $NN$  interaction and off-shell effects.

#### IV. RELATIVISTIC LIPPMANN-SCHWINGER EQUATIONS FOR SPIN-1

A more realistic description of deuteron-nucleus scattering must necessarily involve the use of a scattering equation that describes the propagation of the deuteron pole in the two-nucleon amplitude in the presence of external interactions with the nucleus. Furthermore, we note that to define precisely the relativistic folding procedure one would have to consider the Feynman amplitude for deuteron elastic scattering where the interactions between the nucleons in the deuteron, immediately near the initial and the final states are not present [11]. Considering the restriction to the ladder diagrams a typical contribution to this amplitude is represented in Fig. 1 where the interaction between one nucleon in the deuteron and the nucleus is represented by the Dirac phenomenology optical potential. The resulting  $T_d$  matrix, represented in Fig. 2, can be written in a closed-operator form as

$$T_d = V_d + V_d G T_d, \quad (4.1)$$

where the Green function  $G$  is the product of the full two-particle Green function for the two nucleons in the deuteron by the nucleus propagator and  $V_d$  is the sum of the interactions  $V_1 + V_2$  that are external to the deuteron.

In order to obtain the deuteron optical potential it is necessary to isolate in the two-nucleon propagator the contribution which comes from the deuteron bound state in Hilbert space as explained in Appendix B. The resulting expression for the full two-nucleon propagator is

$$G(P, p', p) = \frac{R(P, p', p)}{P^2 - M_d^2 + i\epsilon} + M(P, p', p), \quad (4.2)$$

where  $M$  is finite when  $P^2 = M_d^2$  and the residue  $R$  is given by

$$R(P, p', p) = \sum_{m=-1,0,1} \left[ \frac{(E + P^0)}{2E} \psi_{P,m} \tilde{\psi}_{P,m} + \frac{(E - P^0)}{2E} \psi_{-P,m} \tilde{\psi}_{-P,m} \right]. \quad (4.3)$$

The amplitudes  $\psi_{P,m}$  and  $\psi_{-P,m}$  are the Fourier transforms of the deuteron and antideuteron Bethe-Salpeter amplitudes, defined in Appendix B, and  $m$  is the spin pro-

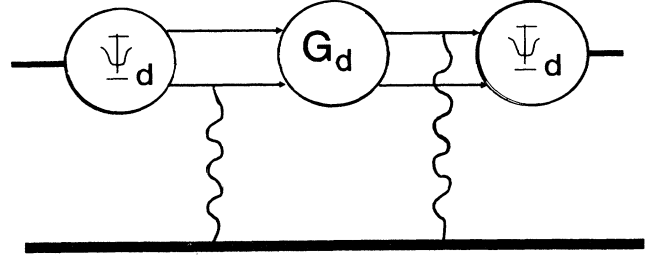


FIG. 1. Diagrammatic representation of one term that contributes to deuteron-nucleus scattering.  $G_d$  is the propagator of the two nucleons in the deuteron which contains, besides the free propagation, all the iterations of the two-nucleon interaction.  $\Psi_d$  are the deuteron wave functions obtained in the residue of the previous propagator at the deuteron-mass pole. The thick line represents the propagation of a spin-zero nucleus taken effectively as a single particle. The wiggling lines represent nucleon-nucleus interactions, and the nucleon propagators are represented by solid lines.

jection. The definition of  $R$  outside the deuteron mass shell is ambiguous due to the presence of  $M$  in Eq. (4.2). Also, this way of splitting the two-nucleon amplitude is only covariant, for the off-mass-shell case, if  $R$  becomes independent of  $E$ . This energy dependence arises even in the calculation of the propagator of elementary particles of spin greater than  $\frac{1}{2}$  and must be solved by redefining the propagator in the off-mass-shell case [12] which, as we have seen, is fully justifiable if one considers bound-state propagation.

The meaning of the operator  $M$  can be understood as the relativistic analogue of the propagation of the two-nucleon asymptotic states associated with the wave functions  $\psi_p^+$ . Following this analogy with nonrelativistic scattering theory [13] we can insert a covariant decomposition of the two-nucleon Green function in Eq. (4.2) into Eq. (4.1), and obtain a pair of equations which define the optical potential scattering equations,

$$T_d = U_d + \int \frac{d^4 P}{(2\pi)^4} U_d \frac{R(P)}{P^2 - M_d^2 + i\epsilon} T_d, \quad (4.4)$$

$$U_d = V_d + \int \frac{d^4 P}{(2\pi)^4} V_d M(P) U_d, \quad (4.5)$$

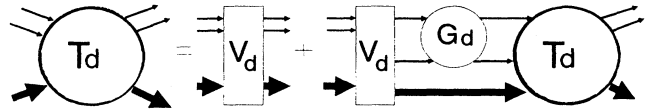


FIG. 2. The Lippmann-Schwinger equation for the  $T$  matrix in the deuteron-nucleus scattering channel. The interactions external to the deuteron are grouped in  $V_d$ . The thick and thin lines represent the propagation of the nucleus and the nucleons, respectively, and  $G_d$  has the same meaning as in Fig. 1.

where we have neglected the recoil of the nucleus. The different models used to calculate the optical potentials correspond to different approximations for  $M(P)$ .

Using the fact that the matrix  $R(P)$  in Eq. (4.4) pro-

jects the intermediate states onto the deuteron bound-state wave function and performing a similar projection on the initial and final states, we obtain a Lippmann-Schwinger equation given by

$$\langle P', m' | T_d | P, m \rangle = \langle P', m' | U_d | P, m \rangle + \sum_{m''} \int \frac{d^4 P''}{(2\pi)^4} \frac{\langle P', m' | U_d | P'', m'' \rangle}{P''^2 - M_d^2 + i\epsilon} \langle P'', m'' | T_d | P, m \rangle, \quad (4.6)$$

where, to simplify the notation, we dropped the subscript  $d$  from  $P$  and  $m$ . It is assumed that the matrix elements in Eq. (4.6) are calculated with the relativistic generalization of the nonrelativistic deuteron internal wave function used in Ref. [6]. The integral over  $d^4 P$  in Eq. (4.6) reduces to a three-dimensional integration over the space-like components since the potential  $U_d$  involves a factor  $2\pi\delta(P'^0 - P^0)$  resulting from the time independence of the Dirac optical potentials. The denominator  $P^2 - M_d^2 + i\epsilon$  can be written as  $\mathbf{K}^2 - \mathbf{P}^2 + i\epsilon$ , where  $K$  verifies the relation  $\mathbf{K}^2 = P_0^2 - M_d^2$ . Both the deuteron bound-state propagator and the matrix elements in Eq. (4.6), calculated for deuteron states of definite momentum and spin projection, do not have a covariant form. However, this form can be achieved by expressing, simultaneously, the interaction and the deuteron states in a covariant spin-1 formalism. For the particular case of the deuteron-nucleus interaction the covariant quantities would have to satisfy the condition

$$\langle P', m' | U_d | P, m \rangle = \epsilon(P', m')_\alpha U^{\alpha\beta} \epsilon(P, m)_\beta, \quad (4.7)$$

where  $\epsilon(P', m')_\alpha$  represents the spin-1 states [2]. On the mass shell the spin-1 projectors must satisfy the relation

$$\epsilon(P', m')_\alpha G(1)^{\alpha\beta} \epsilon(P, m)_\beta = \frac{\delta_{m, m'}}{P^2 - M_d^2 + i\epsilon}, \quad (4.8)$$

where  $G(1)$  is the covariant spin-1 propagator of the Proca equation. The off-mass-shell extension of the potential  $U_d$  is not determined by Eq. (4.7) and depends on the model used to describe the spin-1 field. A similar ambiguity is already present in Eq. (4.2). The way to solve the problem would be to consider the exact off-mass-shell expression for  $M(P)$  that results from the Bethe-Salpeter amplitude once expressed in a covariant form.

## V. BEYOND THE IMPULSE APPROXIMATION

In this section we consider various approximations to the scattering equation in the context of the relativistic formalism. It is important to realize that the requirements imposed by multiple-scattering theory on the calculation of the deuteron optical potential are much stronger in the relativistic than in the nonrelativistic approach. The reason is that the scalar and vector interactions have larger strengths than the nonrelativistic central and spin-orbit potentials. Therefore, expressions valid only in first order on the potential become even more

questionable in the relativistic treatment. Furthermore, it is less justifiable to neglect intermediate states far off in energy because  $S$  and  $V$  produce strong spin-dependent interactions and low effective masses that induce a significant coupling between positive- and negative-energy spinor states.

The simplest approximation based on Eq. (4.5) results from neglecting the term involving  $M(P)$ . This gives  $U_d = V_d$  which after insertion into Eq. (4.4) leads to an effective optical potential scattering equation. The relativistic folding model of deuteron-nucleus scattering corresponds to the assumption that  $V_d$  is given by Eqs. (2.4), (2.5), and (2.6).

A straightforward improvement would be to include the  $M(p)$  term of the two-nucleon propagator in the scattering calculation using Eq. (4.1). In order to implement this approach one must also use an approximate method to perform the integration in the continuum of the two-nucleon scattering states [14]. The Faddeev equations can also be used as a basis for this type of calculation [15]. Both approaches go beyond optical potential scattering and formally provide an exact description within the framework of a three-body problem. The relativistic analogue would involve the coupling to the negative-energy components in both the bound and scattering states. Furthermore, we have to take into account the fact that the two-nucleon center-of-mass frame is changing during the scattering process, thereby requiring a fully covariant formalism.

A different way to proceed is to improve the calculation of the optical potential in Eq. (4.5). Introducing the Watson single-scattering operator we can isolate in Eq. (4.5) the infinite series that involves only the nucleon-nucleus potential [13],

$$\tau_i = V_i + V_i M \tau_i, \quad (5.1)$$

where  $i$  represents the proton or the neutron and  $M$  is given by Eq. (4.2). The deuteron-nucleus optical potential can then be written as the iteration of this operator applied successively to the different nucleons in the deuteron,

$$U_d = (\tau_1 + \tau_2) + (\tau_1 M \tau_2 + \tau_2 M \tau_1) + (\tau_1 M \tau_2 M \tau_1 + \tau_2 M \tau_1 M \tau_2) + \dots \quad (5.2)$$

The relativistic impulse approximation results from keeping only the first-order term in this equation and approximating  $M$  in Eq. (5.1) by the free-nucleon propagator. Therefore the operators  $\tau_{1,2}$  become equal to the

nucleon-nucleus  $T$  matrix  $T_i$ . Two different assumptions are involved: the two-nucleon amplitude with the deuteron pole subtracted is approximated by the free propagation of the two nucleons; rescattering involving the two nucleons in the deuteron is ignored.

Within this framework the direct impulse approximation is obtained by neglecting the deuteron-pole term in Eq. (4.4). This implies that  $T_d = U_d = T_1 + T_2$  thereby reproducing Eq. (3.8).

## VI. NONRELATIVISTIC FOLDING IN MOMENTUM SPACE OF THE DIRAC EQUIVALENT POTENTIALS

Deuteron-nucleus scattering at intermediate energies has been analyzed using the conventional nonrelativistic folding model where the nucleon-nucleus interaction is represented as the sum of a central and a spin-orbit potential. Recently Yahiro *et al.* [16] performed this type of analysis using different shapes and parametrizations for the nucleon potentials. Better agreement with experiment is obtained using wine-bottle-shaped nucleon optical potentials derived from the reduction to Schrödinger form of the Dirac equation with scalar plus vector potentials, than with standard Woods-Saxon potentials. Both types of nucleon-nucleus optical potentials reproduce the proton-scattering data equally well. Furthermore, they find that discrepancies between theory and experiment for  $\theta \geq 15^\circ$  can be attributed to deuteron breakup effects.

We shall compare here the relativistic models of deuteron-nucleus scattering with the nonrelativistic folding model using potentials derived from the Dirac phenomenology. The particular shape and parametrization of these potentials improves the fit to experiment but does not correspond to a coherent method to include relativistic effects in deuteron-nucleus scattering. In order to make the comparisons meaningful we use in all calculations the same nucleon-nucleus scalar and vector potentials.

Since the calculations for the relativistic models of deuteron-nucleus scattering are performed in momentum space, it is convenient to express the nonrelativistic folding in the same way. In momentum space the nucleon-nucleus interaction can be written as

$$V_{nr} = V_c(q) + iV_{s.o.}(q)\sigma \cdot \mathbf{p}' \times \mathbf{p}, \quad (6.1)$$

where  $\sigma$  are the Pauli matrices.  $V_c(q)$  is, of course, the Fourier transform of the central part of the potential in configuration space given by

$$V_c(r) = S(r) + \frac{E}{m}V(r) + \frac{1}{2m}[S(r)^2 - V(r)^2]. \quad (6.2)$$

As regards the spin-orbit part of the interaction we note that [6]  $V_{s.o.}(q)$  is the Fourier transform of a function  $V_{Ds.o.}$  which is related to the nucleon-nucleus spin-orbit interaction  $V_{s.o.}(r)$  in configuration space by

$$V_{s.o.}(r) = \frac{1}{r} \frac{dV_{Ds.o.}(r)}{dr}. \quad (6.3)$$

Since the spin-orbit part in configuration space is

$$V_{s.o.}(r) = \frac{1}{2m[E + m + S(r) - V(r)]} \frac{1}{r} \frac{d}{dr} [V(r) - S(r)], \quad (6.4)$$

we conclude that

$$V_{Ds.o.}(r) = \frac{V(r) - S(r)}{2m[E + m + S(r) - V(r)]} + \int_r^\infty dr' \frac{[V(r') - S(r')](d/dr)[V(r') - S(r')]}{\{2m[E + m + S(r') - V(r')]\}^2}. \quad (6.5)$$

Using Eq. (6.1) and performing the folding over the deuteron internal wave function  $\psi(\mathbf{p})$ , assumed to be a pure  ${}^3S_1$  state, the deuteron-nucleus effective interaction in momentum space is given by

$$U_d(q) = 2 \int \frac{d^3p}{(2\pi)^3} \psi^* \left[ \mathbf{p} - \frac{\mathbf{q}}{2} \right] \left[ V_c(q) + iV_{s.o.}(q)\mathbf{J} \cdot \left[ \frac{\mathbf{p}}{2} - \mathbf{p} + \mathbf{q} \right] \times \left[ \frac{\mathbf{p}}{2} - \mathbf{p} \right] \right] \psi(\mathbf{p}), \quad (6.6)$$

where  $\mathbf{J}$  is the spin-1 operator. After integration over the deuteron internal momentum only the term in  $\mathbf{p}' \times \mathbf{p}$  survives in the spin-orbit part of the interaction since  $\mathbf{q} \times \mathbf{p}$  gives a vanishing contribution. The resulting deuteron-nucleus effective potential has the form of Eq. (2.4) with

$$U_c(q) = 2\rho V_c(q), \quad (6.7)$$

$$U_{s.o.}(q) = \rho V_{s.o.}(q), \quad (6.8)$$

where  $\rho$  is the deuteron probability density.

## VII. CALCULATIONS

In order to compare the various relativistic formalisms of deuteron-nucleus scattering developed here with the

nonrelativistic approach we performed calculations of the cross section and polarization observables for  ${}^{40}\text{Ca}$  and  ${}^{58}\text{Ni}$  targets at energies where data are presently available [17]. Three different approximations are considered in the relativistic case.

In the relativistic folding model (model I) the deuteron-nucleus effective interaction is represented by the relativistic folding of the nucleon-nucleus scalar and vector Dirac optical potentials. The central and spin-orbit parts of this interaction in momentum space are given by Eqs. (2.5) and (2.6) in terms of  $S$  and  $V$ . To calculate the deuteron scattering observables we use the Schrödinger equation, modified in order to take into account relativistic kinematics.

In the direct impulse approximation (model II) the

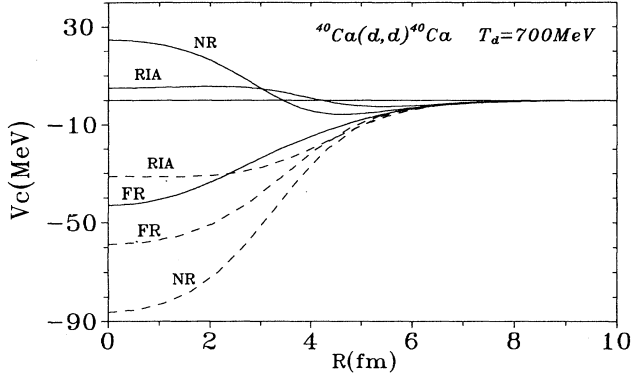


FIG. 3. The  $d$ - $^{40}\text{Ca}$  central optical potential at 700 MeV. The real part is represented by the solid curves while the dashed curves represent the imaginary part. The results correspond to relativistic folding of the scalar and vector optical potentials obtained in Dirac phenomenology, FR (model I); folding of the two relativistic nucleon-nucleus  $T$  matrices, RIA (model III); folding of the effective nonrelativistic potentials obtained from the nucleon-nucleus Dirac optical potentials, NR.

deuteron-nucleus scattering amplitude is obtained by folding the sum of the nucleon-nucleus  $T$  matrices which result from solving the nucleon-nucleus Dirac equation. These  $T$  matrices have the form of Eq. (3.3) where  $T_0$  and  $T_s$  are given by Eqs. (3.6) and (3.7). Finally in the relativistic impulse approximation (model III) the Fourier transform of the deuteron-nucleus  $T$  matrix of model II is used as the effective interaction in the deuteron Schrödinger equation.

To make the comparison meaningful we used the same parameters for the Dirac potentials and the same deuteron bound-state wave function in all the calculations. The Dirac optical potentials used were obtained from the global potentials for  $^{40}\text{Ca}$  of fit I in Ref. [10]. The energy at which both the Dirac optical potential and the nucleon-nucleus  $T$  matrix are calculated is half the deuteron energy. In the case of  $^{58}\text{Ni}$  the geometry of the global

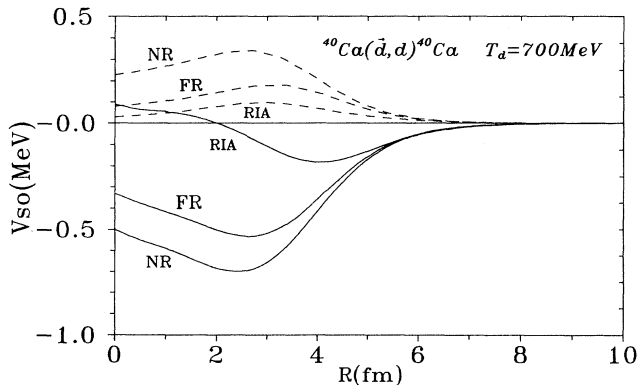


FIG. 4. The curves of the real (solid) and imaginary (dashed) parts of the spin-orbit potential corresponding to the same models as in Fig. 3.

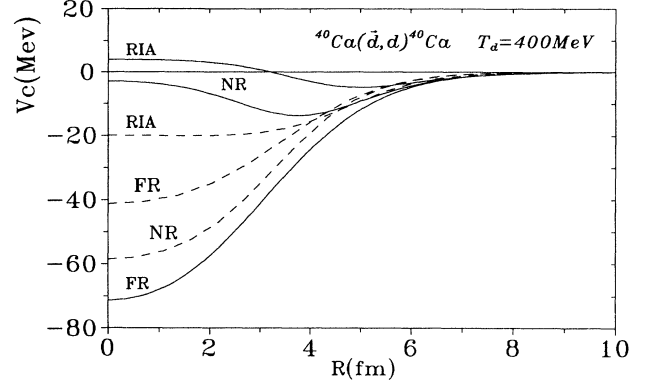


FIG. 5. The same as Fig. 3 for a deuteron energy of 400 MeV.

potentials was scaled from that of  $^{40}\text{Ca}$  using the  $r=r_0 A^{1/3}$  dependence. The radial part of the  $^3S_1$  deuteron bound state was represented by a Yamaguchi [18] wave function. The deuteron probability densities were first calculated in configuration space and then Fourier transformed into momentum space. All Fourier transformations were performed numerically using an adaptive routine designed to integrate oscillating functions.

The deuteron-nucleus scattering equation was solved using the eikonal approximation. Good agreement was obtained in comparisons between the results of the eikonal approximation and conventional optical model programs. In order to take into account relativistic kinematics the reduced mass was given by [19]

$$\mu = \frac{M_d E_N}{E_d + E_N}, \quad (7.1)$$

where  $E_d, E_N$  are the deuteron and the target nucleus center-of-mass energies. Consequently, the Coulomb potential had to be corrected by a factor of  $E_d/M_d$  to make it compatible with the relativistic expression of the Coulomb cross section. The charge density used for  $^{58}\text{Ni}$  and  $^{40}\text{Ca}$  was obtained by fitting a Fermi distribution to

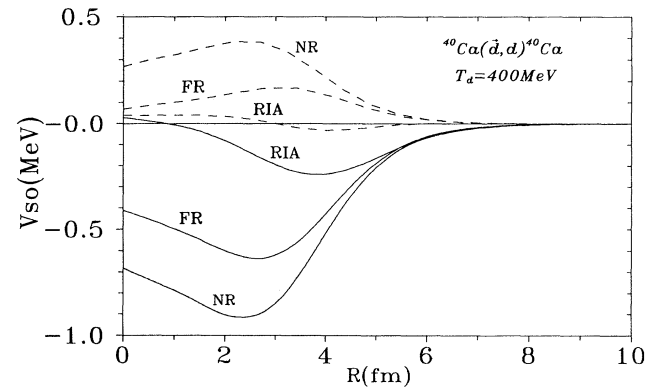


FIG. 6. The same as Fig. 4 for a deuteron energy of 400 MeV.

electron-scattering data [20].

Figures 3–6 represent the effective deuteron-nucleus potential in models I and III and in the nonrelativistic folding model. We note that the real central potential in the relativistic folding model does not have the characteristic wine-bottle shape. This results from the absence of the quadratic terms in  $S$  and  $V$ . Furthermore, we note that the strength of the potential in the relativistic impulse approximation tends to be weaker than in the relativistic and the nonrelativistic folding models. Figures 7–11 show the results of calculations for deuteron-nucleus scattering from  $^{40}\text{Ca}$  and  $^{58}\text{Ni}$  at deuteron energies of 400 and 700 MeV.

### VIII. CONCLUSIONS

Within the group of relativistic models we find that the direct impulse approximation provides the most satisfactory description of the experimental data. However detailed agreement, especially as regards  $A_{yy}$ , is not very good. The magnitude of  $A_y$  is well predicted in the direct impulse approximation but  $A_{yy}$  tends to be systematically smaller than experiment. Furthermore, we note a shift in the position of the predicted minima and generally better agreement at the higher energy. It should be noted that we did not try to improve the fit to experiment by variation of the parameters in the optical model potentials, since our main objective was to determine the reliability of a microscopic theory of deuteron-

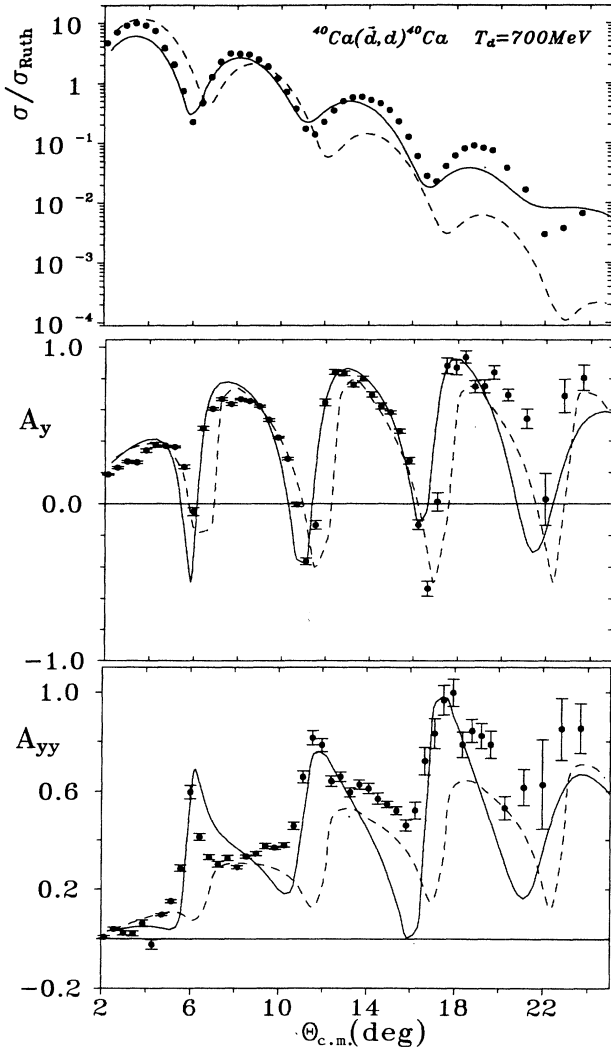


FIG. 7. Calculations for the cross section, in units of  $\sigma_{\text{Ruth}}$ , vector analyzing power  $A_y$ , and tensor analyzing power  $A_{yy}$  for  $d\text{-}^{40}\text{Ca}$  scattering at 700 MeV. The solid curves were obtained with the nonrelativistic folding model (NR), and the broken curves with the direct impulse approximation (model II). The data are from Ref. [17].

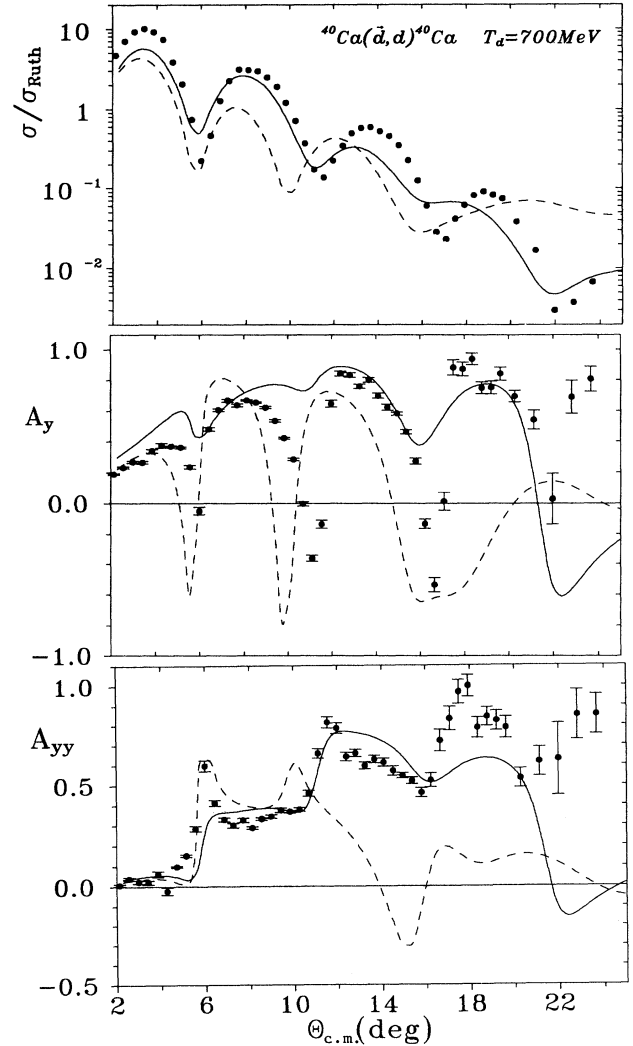


FIG. 8. Calculations for the same data as in Fig. 7 using the relativistic folding model (model I)—solid curves—and the relativistic impulse approximation (model III)—broken curves.



nucleus scattering based on global nucleon-nucleus potentials that reproduce proton-nucleus elastic scattering.

The results of calculations using the relativistic models I and III, shown in Fig. 8, give a very unsatisfactory description of the data particularly in the case of the relativistic folding of the Dirac potentials. This is probably a consequence of the fact that the effective potential does not include a quadratic dependence on  $S$  and  $V$ . The failure of models I and III is likely to be a reflection of the inadequate treatment of multiple-scattering effects. It is understandable that multiple scattering will play a much more crucial role in the relativistic than in the non-relativistic approach. This is a consequence of the fact that the relativistic proton-nucleus scalar and vector potentials are much stronger than the central and spin-orbit potentials. Furthermore, the important contribution of

the negative-energy states implies that we cannot neglect intermediate states in the scattering process based on the argument that their energies are far away from the initial- and final-state nucleon energies. Future relativistic calculations of deuteron-nucleus scattering at intermediate energies should include a more realistic treatment of multiple-scattering effects and also a fully covariant description of the deuteron amplitudes.

Calculations with the nonrelativistic folding model give a reasonable description of the cross section and polarization observables for  $^{40}\text{Ca}$  and  $^{58}\text{Ni}$  at both energies. We may expect that better-detailed agreement with experiment could be obtained with the inclusion of deuteron breakup effects [14]. We emphasize that the use of Dirac  $S$  and  $V$  potentials to generate the nucleon-nucleus effective interaction constitutes a convenient form of pa-

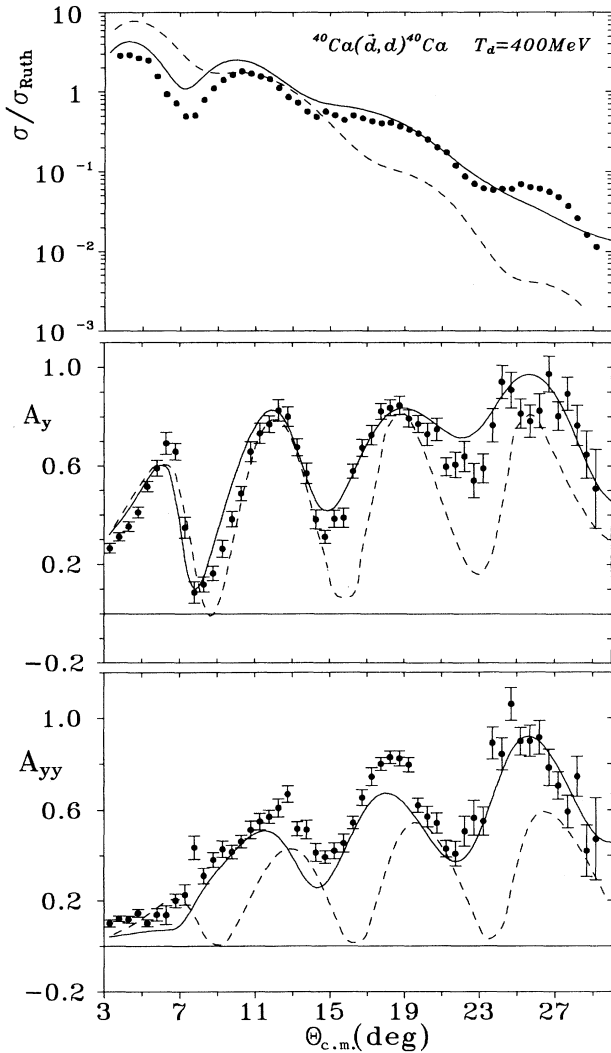


FIG. 9. Calculations of the same observables as in Fig. 7 for  $d\text{-}^{40}\text{Ca}$  scattering at 400 MeV. The solid and broken curves have the same meaning as in Fig. 7.

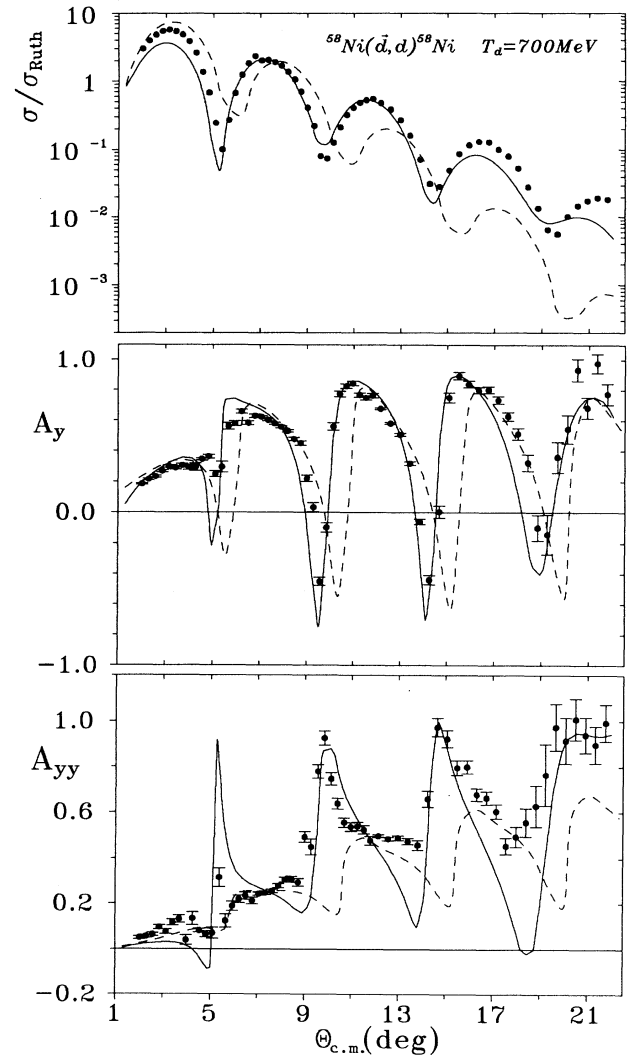


FIG. 10. Calculations of the same observables as in Fig. 7 for  $d\text{-}^{58}\text{Ni}$  scattering at 700 MeV. The curves have the same meaning as in Fig. 7.

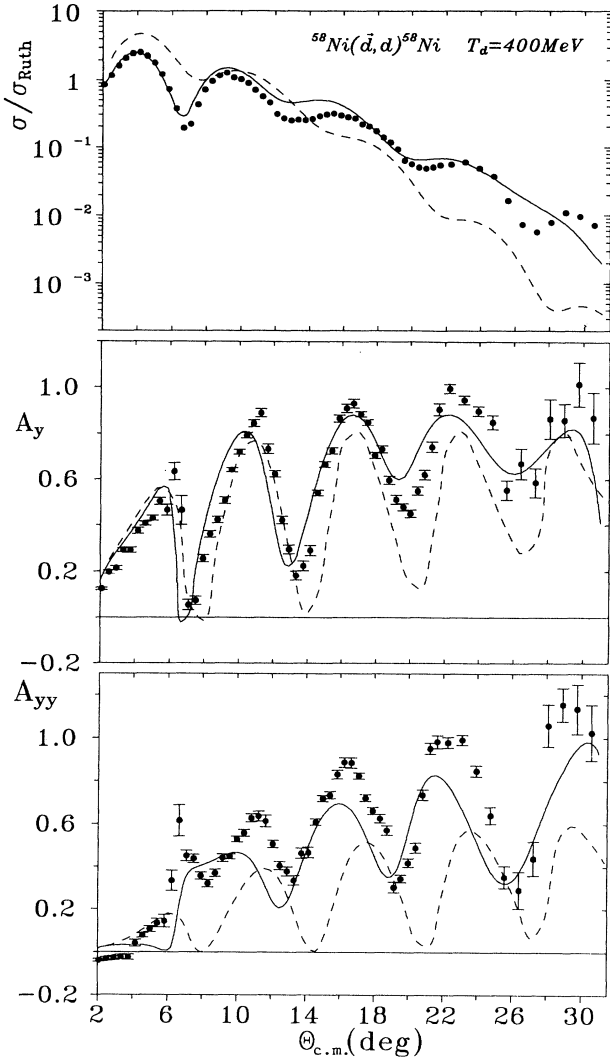


FIG. 11. Calculations of the same observables as in Fig. 7 for  $d\text{-}^{58}\text{Ni}$  scattering at 400 MeV. The curves have the same meaning as in Fig. 7.

rametrization, but does not qualify the model as a coherent relativistic model.

Finally we note that the impulse approximation represents an improvement over the description of

deuteron-nucleus scattering using one-body spin-1 relativistic equations since it includes explicitly the structure of the deuteron. Furthermore, the model provides a reasonable description of the cross section and polarization observables in the Saclay data [17]. However, a microscopic relativistic theory which may be capable of providing detailed agreement with deuteron-nucleus scattering data at intermediate energies requires considerable improvement of the direct impulse approximation.

#### ACKNOWLEDGMENTS

The authors acknowledge useful discussions with Edward F. Redish, M. Yahiro, S. J. Wallace, and P. J. A. Bicudo. This work was supported by the Instituto Nacional de Investigação Científica.

#### APPENDIX A: EXPRESSION OF THE OBSERVABLES IN TERMS OF $T_s$ AND $T_0$

The relation between the Feynman amplitude  $\mathcal{T}$  for the nucleon-nucleus scattering and the corresponding center-of-mass differential cross section is

$$\frac{d\sigma_{if}}{d\Omega_{c.m.}} = \frac{(2m)^2}{64\pi^2 s} |\mathcal{T}_{if}(s, t)|^2. \quad (\text{A1})$$

This relation can be written in the nonrelativistic form

$$\frac{d\sigma_{if}}{d\Omega_{c.m.}} = \frac{\mu^2}{(2\pi)^2} |T_{if}(s, t)|^2, \quad (\text{A2})$$

where  $T = \mathcal{T}/(2E_N)$  and  $\mu = mE_N/(E_p + E_N)$  corresponds to the reduced mass. The factor  $2E_N$  removes the covariant normalization for the spin-zero target nucleus since we are considering an effective one-body Dirac equation. The cross sections for spin up  $\sigma^{\text{up}}$  and spin down  $\sigma^{\text{down}}$  relative to the scattering plane are given in terms of the  $T$  matrix (3.3) by

$$\sigma^{\text{up/down}} = \frac{(mE_N)^2}{8\pi^2 s} \text{Tr} \left[ T \frac{\not{n} + m}{2} \frac{1 \pm \gamma^5 \not{n}}{2} \bar{T} \frac{\not{n}' + m}{2} \right], \quad (\text{A3})$$

where  $n^\mu$  is the spacelike unitary vector  $(0, \mathbf{n})$ . Expressed in terms of  $T_s$  and  $T_0$  the cross section  $\sigma$  and the vector analyzing power  $A_y$  are given by

$$\begin{aligned} \sigma &= \sigma^{\text{up}} + \sigma^{\text{down}} \\ &= \frac{E_N^2}{8\pi^2 s} [(E_p^2 + m^2)(|T_s|^2 + |T_0|^2) + 2mE_p(T_s T_0^* + T_0 T_s^*) + D(|T_0|^2 - |T_s|^2)], \end{aligned} \quad (\text{A4})$$

$$\begin{aligned} A_y &= (\sigma^{\text{up}} - \sigma^{\text{down}}) / \sigma \\ &= \frac{-iC(T_0 T_s^* - T_s T_0^*)}{(E_p^2 + m^2)(T_s T_s^* + T_0 T_0^*) + 2mE_p(T_s T_0^* + T_0 T_s^*) + D(T_0 T_0^* - T_s T_s^*)}, \end{aligned} \quad (\text{A5})$$

from which one can obtain the nonrelativistic expressions for the observables by replacing  $T_s, T_0$  as a function of  $T_f, T_g$  according to Eqs. (3.6) and (3.7).

## APPENDIX B: THE DEUTERON POLE APPROXIMATION OF THE TWO-NUCLEON AMPLITUDE

The projection operator over the deuteron and antideuteron, expressed in terms of states which transform covariantly under the Poincaré group, with definite mass and spin is given by

$$\Lambda_d = \sum_m \int \frac{d^3P}{(2\pi)^3 2E_d(P)} (|P, m_d\rangle \langle P, m_d| + |\overline{P}, m_d\rangle \langle \overline{P}, m_d|) . \quad (B1)$$

Thus the two-nucleon propagator

$$iG(x'_1, x'_2; x_1, x_2) = \langle 0 | T \psi(x'_1) \psi(x'_2) \bar{\psi}(x_1) \bar{\psi}(x_2) | 0 \rangle \quad (B2)$$

is

$$iG(x'_1, x'_2; x_1, x_2) = \sum_m \int \frac{d^3P}{(2\pi)^3 2E_d(P)} \psi_{P,m} \bar{\psi}_{P,m} \theta(X'^0 - X^0) + \psi_{-\overline{P},m} \bar{\psi}_{-\overline{P},m} \theta(X^0 - X'^0) + M , \quad (B3)$$

where the Bethe-Salpeter amplitudes are defined by

$$\psi_{P,m} = \langle 0 | T \psi(x'_1) \psi(x'_2) | P, m \rangle , \quad (B4)$$

$$\bar{\psi}_{P,m} = \langle P, m | T \bar{\psi}(x_1) \bar{\psi}(x_2) | 0 \rangle , \quad (B5)$$

$$\psi_{-\overline{P},m} = \langle \overline{P}, m | T \psi(x_1) \psi(x_2) | 0 \rangle , \quad (B6)$$

$$\bar{\psi}_{-\overline{P},m} = \langle 0 | T \bar{\psi}(x'_1) \bar{\psi}(x'_2) | \overline{P}, m_d \rangle , \quad (B7)$$

and,  $X, X'$  are the average coordinates in the initial and final states, given by  $X = (x_1 + x_2)/2$  and  $X' = (x'_1 + x'_2)/2$ . The term  $M$  contains all the contributions from other states in the Hilbert space and from the

time-ordering rearrangements which are different from those present explicitly in Eq. (B3). These contributions will be finite near the deuteron pole and, therefore, are only relevant when the deuteron is off mass shell. Introducing the representation of the  $\theta$  function given by

$$\theta(t) = \int \frac{dw}{2\pi i} \frac{e^{iwt}}{w - i\epsilon} , \quad (B8)$$

with  $p^0 = E_d - w$  and  $p^0 = w - E_d$ , in the first and second terms of the second member of Eq. (B3), one obtains in the momentum space the representation of the two-nucleon propagator given in Eqs. (4.2) and (4.3).

- 
- [1] B. C. Clark, R. L. Mercer, and P. Schwandt, Phys. Lett. **122B**, 211 (1983).
  - [2] F. D. Santos and H. van Dan, Phys. Rev. C **34**, 250 (1986).
  - [3] R. E. Kozack, B. C. Clark, S. Hama, V. K. Mishra, G. Kälbermann, R. L. Mercer, and L. Ray, Phys. Rev. C **37**, 2898 (1988).
  - [4] R. E. Kozack, B. C. Clark, S. Hama, V. K. Mishra, R. L. Mercer, and L. Ray, Phys. Rev. C **40**, 2181 (1989).
  - [5] V. K. Mishra, S. Hama, B. C. Clark, R. E. Kozack, R. L. Mercer, and L. Ray, Phys. Rev. C **43**, 801 (1991).
  - [6] F. D. Santos and A. Amorim, Phys. Rev. C **37**, 1183 (1988).
  - [7] J. A. McNeil, J. R. Shepard, and S. J. Wallace, Phys. Rev. Lett. **50**, 1470 (1984).
  - [8] J. A. Tjon and S. J. Wallace, Phys. Rev. C **36**, 1085 (1987).
  - [9] Neil A. Ottenstein, Joseph Sabutis, and Stephen J. Wallace, Phys. Rev. C **35**, 369 (1987).
  - [10] E. D. Cooper, B. C. Clark, R. E. Kozack, S. Shim, S. Hama, J. I. Johansson, H. S. Sherif, R. L. Mercer, and B. D. Serot, Phys. Rev. C **36**, 2170 (1987).
  - [11] Kerson Huang and H. Arthur Weldon, Phys. Rev. D **11**, 257 (1975).
  - [12] Steven Weinberg, Phys. Rev. **133**, B1318 (1964).
  - [13] P. C. Tandy, Edward F. Redish, and D. Bollé, Phys. Rev. C **16**, 1924 (1977).
  - [14] N. Austern, Y. Iseri, M. Kamimura, M. Kawai, G. Rawitscher, and M. Yahiro, Phys. Rep. **154**, 125 (1987).
  - [15] Sadhan K. Adhikari, Ann. Phys. (N.Y.) **163**, 149 (1985).
  - [16] M. Yahiro, H. Kameyama, M. Kamimura, and M. Kawai, Phys. Lett. B **182**, 135 (1986).
  - [17] Nguyen Van Sen, J. Arvieux, Ye Yanlin, G. Gailard, B. Bonin, A. Boudard, G. Bruge, J. C. Lugol, R. Rabinet, T. Hasegawa, F. Soga, J. M. Cameron, G. C. Neilson, and D. M. Sheppard, Phys. Lett. B **156**, 185 (1985).
  - [18] Yoshio Yamaguchi, Phys. Rev. **95**, 1628 (1954).
  - [19] A. Ingemarsson, Phys. Scr. **9**, 156 (1974).
  - [20] C. W. Jager, H. de Vries, and C. de Vries, At. Data Nucl. Data Tables **14**, 479 (1974).